$$\begin{bmatrix} \tilde{\tilde{\mathbf{e}}}(k_s, z_M^-) \\ \tilde{\tilde{\mathbf{h}}}(k_s, z_M^-) \end{bmatrix} = \overline{M}_1 \cdot \overline{M}_2 \cdot \overline{M}_3 .... \overline{M}_M \cdot \begin{bmatrix} \tilde{\tilde{\mathbf{e}}}(k_s, 0) \\ \tilde{\tilde{\mathbf{h}}}(k_s, 0) \end{bmatrix} \quad (11)$$

Above the patches interface, the relation between the tangential electric and magnetic fields components in dielectric layers is given by:

$$\begin{bmatrix} \tilde{\tilde{\mathbf{e}}}(k_s, z_N^+) \\ \tilde{\tilde{\mathbf{h}}}(k_s, z_N^+) \end{bmatrix} = \overline{M}_{M+1} \cdot \overline{M}_{M+2} \cdot \overline{M}_{M+3} .... \overline{M}_N \cdot \begin{bmatrix} \tilde{\tilde{\mathbf{e}}}(k_s, z_M^+) \\ \tilde{\tilde{\mathbf{h}}}(k_s, z_M^+) \end{bmatrix} \quad (12)$$

We can put the product matrix as:

$$\overline{\Gamma}_< = \prod_{j=M}^{1} \overline{M}_j = \begin{bmatrix} \Gamma_<^{11} & \Gamma_<^{12} \\ \Gamma_<^{21} & \Gamma_<^{22} \end{bmatrix} \quad (13)$$

and

$$\overline{\Gamma}_> = \prod_{j=N}^{M+1} \overline{M}_j = \begin{bmatrix} \Gamma_>^{11} & \Gamma_>^{12} \\ \Gamma_>^{21} & \Gamma_>^{22} \end{bmatrix} \quad (14)$$

Where $\prod_{j=M}^{1}$ and $\prod_{j=N}^{M+1}$ means the multiplication of matrices above and below the patches.

By using the boundary conditions and condition of continuity of E and H fields, we can find that the relationship between the patch current and the electric field on the patch is given by [8]:

$$\tilde{\tilde{\mathrm{E}}}(\mathrm{k_s}) = \overline{\mathrm{G}}(\mathrm{k_s}) \cdot \tilde{\tilde{\mathrm{J}}}(\mathrm{k_s}) \quad (15)$$

Where $\tilde{\mathrm{J}}(\mathrm{k_s})$ is the current on the patch, and $\overline{\mathrm{G}}$ is the spectral dyadic Green’s function, its expression is shown to be given by:

$$\overline{\mathrm{G}}(\mathrm{k_s}) = \begin{bmatrix} \mathrm{G_{xx}} & \mathrm{G_{xy}} \\ \mathrm{G_{yx}} & \mathrm{G_{yy}} \end{bmatrix} = \frac{1}{\mathrm{k_s^2}} \cdot \begin{bmatrix} \mathrm{k_x} & \mathrm{k_y} \\ \mathrm{k_y} & -\mathrm{k_x} \end{bmatrix} \cdot \overline{\mathrm{Q}} \cdot \begin{bmatrix} \mathrm{k_x} & \mathrm{k_y} \\ \mathrm{k_y} & -\mathrm{k_x} \end{bmatrix} \quad (16)$$

Where Q is given by:

$$Q(k_s) = -(\overline{\Gamma}_<)_{12} \cdot [\overline{g}_0 \cdot (\overline{\Gamma}_>)_{12} - (\overline{\Gamma}_>)_{22}] \cdot [\overline{g}_0 \cdot (\overline{\Gamma})_{12} - (\overline{\Gamma})_{22}]^{-1} \quad (17)$$

The surface current $\overline{\mathrm{J}}(\mathrm{r_s})$ on the patch can be expanded into a finite series of known basis functions $\mathrm{J_{xn}}$ and and $\mathrm{J_{yn}}$. [9]:

$$\overline{\mathrm{J}}(\mathbf{r}_s) = \sum_{n=1}^{N} a_n \begin{bmatrix} J_{xn}(\mathbf{r}_s) \\ 0 \end{bmatrix} + \sum_{m=1}^{M} b_m \begin{bmatrix} 0 \\ J_{ym}(\mathbf{r}_s) \end{bmatrix} \quad (18)$$

Where an and bn are the mode expansion coefficients to be determined in the x and y direction respectively.

The main problem is how to select the basis functions associated with the complete orthogonal set of TM and TE modes of rectangular microstrip antenna (figure 2).

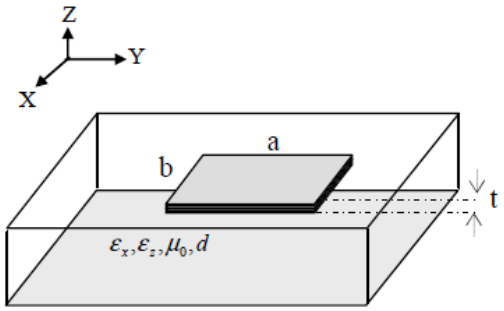

Fig. 2. Geometry of High superconducting rectangular microstrip on uniaxial substrate

To include the effect of the superconductivity of the microstrip antenna in full-wave analysis, the impedance is determined by using London’s equation and the model of Gorter and Gasimir, it is given by [5]:

$$Z_S = R_S + iX_S \quad (19)$$

Where Zs is the surface impedance of the superconducting patch, Rs and Xs are the surface resistance and the surface reactance.

When the thickness (t) of the superconducting patch is less than three times the zero-temperature penetration depth (0 l), the surface impedance can be approximated as follows:

$$Z_S = \frac{1}{t\sigma} \quad (20)$$

Where σ is the complex conductivity of the superconducting film, is given by

$$\sigma = \sigma_1 - i\sigma_2 \quad (21)$$

The conductivity components are given by: $\sigma_1 = \sigma_n (T/T_c)^4$ and $\sigma_2 = \frac{1-(T/T_c)^4}{\omega \mu_0 \lambda_0^2}$.

Where σ_n: Is the normal state conductivity at $T=T_C$, and ω is the angular frequency.

Enforcement of the boundary conditions requiring that the transverse component of the electric field to vanish on the High superconducting rectangular microstrip, and the current on the patch is then formulated using the dyadic Green’s function.

$$\overline{\mathrm{E}}(\mathrm{r_s}) = \frac{1}{(2\pi)^2} \int \mathrm{dk_s} \cdot \mathrm{F}(\mathrm{k_s}, \mathrm{r_s}) \cdot (\overline{\mathrm{G}}(\mathrm{k_s}) - \overline{\mathrm{Z}}\mathrm{s}) \cdot \tilde{\mathrm{J}}(\mathrm{k_s}) = 0 \quad (22)$$

Where $\overline{\mathrm{Z}}_\mathrm{S} = \begin{vmatrix} \mathrm{Z_s} & 0 \\ 0 & \mathrm{Z_s} \end{vmatrix}$

Substituting (16) into (22) and using the selected basis functions as testing functions, we obtain the following homogeneous matrix equation:

$$\begin{bmatrix} [\overline{\mathrm{B}}_{\mathrm{kn}}]_{\mathrm{NxN}} & [\overline{\mathrm{B}}_{\mathrm{km}}]_{\mathrm{NxM}} \\ [\overline{\mathrm{B}}_{\mathrm{ln}}]_{\mathrm{MxN}} & [\overline{\mathrm{B}}_{\mathrm{lm}}]_{\mathrm{MxM}} \end{bmatrix} \cdot \begin{bmatrix} [\mathrm{a_n}]_{\mathrm{NX1}} \\ [\mathrm{b_m}]_{\mathrm{MX1}} \end{bmatrix} = \begin{vmatrix} [0]_{\mathrm{NX1}} \\ [0]_{\mathrm{MX1}} \end{vmatrix} \quad (23)$$

Where

$$\overline{B}_{kn} = \int_{-\infty}^{+\infty}\int_{-\infty}^{+\infty} dk_s \frac{1}{k_s^2}(G_{xx} - Z_S)\tilde{J}_{xk}(-k_s)\tilde{J}_{xn}(k_s) \quad (24)$$

$$\overline{B}_{km} = \int_{-\infty}^{+\infty}\int_{-\infty}^{+\infty} dk_s \frac{k_x k_y}{k_s^2} G_{xy}\tilde{J}_{xk}(-k_s)\tilde{J}_{ym}(k_s) \quad (25)$$

$$\overline{B}_{ln} = \int_{-\infty}^{+\infty}\int_{-\infty}^{+\infty} dk_s \frac{k_x k_y}{k_s^2} G_{yx}\tilde{J}_{yl}(-k_s)\tilde{J}_{xn}(k_s) \quad (26)$$

$$\overline{B}_{lm} = \int_{-\infty}^{+\infty}\int_{-\infty}^{+\infty} dk_s \frac{1}{k_s^2}(G_{yy} - Z_S)\tilde{J}_{yl}(-k_s)\tilde{J}_{ym}(k_s) \quad (27)$$

Therefore, for the existence of nontrivial solutions, the determinant of (31) must be zero.

$$\det(\overline{B}(f)) = 0 \quad (28)$$

In general the root of equation (28) is the characteristic equation for the complex resonant frequency $f = f_r + if_i$. f_r is the resonant frequency and $2f_i / f_r$ is the half-power bandwidth of the antenna.

Once the problem is solved for the resonant frequency, far field radiations in spherical coordinates are given from the vector Fourier transform of the electric field.

$$E_x(x,y) = \frac{1}{4.\pi^2}\int_{-\infty}^{+\infty}\int_{-\infty}^{+\infty}[(G_{xx} - Z_S).\tilde{J}_x + G_{xy}.\tilde{J}_y]e^{j(k_x.x+k_y.y)}.dk_x.dk_y \quad (29)$$

$$E_y(x,y) = \frac{1}{4.\pi^2}\int_{-\infty}^{+\infty}\int_{-\infty}^{+\infty}[G_{yx}.\tilde{J}_x + (G_{yy} - Z_S).\tilde{J}_y]e^{j(k_x.x+k_y.y)}.dk_x.dk_y \quad (30)$$

Using the stationary phase method, we can obtain the far-zone, co-polar and cross- polar field components of structure are, respectively given by:

$$E_\phi(\theta,\phi) = -E_x \sin\phi + E_y \cos\phi \quad (31)$$

$$E_\theta(\theta,\phi) = E_x \cos\theta\cos\phi + E_y \cos\theta \sin\phi \quad (32)$$

The electric field component are defined in the interval

$$0 \le \theta \le \pi, \quad 0 \le \phi \le 2\pi$$

An array has many advantages over a single element. A linear array has excellent directivity and it can form the narrowest main-lobe in a given direction [10]-[12]. The total far field of any antenna array with identical radiating elements is the product of the element factor EΘ,ϕ and array factor AF. The AF depends on the geometric arrangement of the array elements, the spacing of the elements, and excitation of each element. By varying the separation Y and/or the phase ψ between the elements, the characteristics of the array factor and the total field of the array can be controlled.

$$F(\theta,\phi) = E_{\theta,\Phi}.AF(\theta,\phi) \quad (33)$$

Where

$$AF(\theta,\phi) = \sum_{k=1}^{2N} A_k \exp(i(k_0 Y_k \sin\theta\cos\phi + \psi_k)) \quad (34)$$

The Excitation coefficients (amplitude and phase) of the N elements are chosen to be: $I_k = A_k e^{j\psi_k}$. Through, to determine the values of parameters (Y_k: distance, and A_k : amplitude), we used particle swarm optimization (PSO) to approximate the radiation pattern function, for getting better the radiation pattern of array. Particle swarm optimization (PSO) was originally developed by Dr. Eberhart and Dr. Kennedy in 1995, inspired by social behavior of swarms. It has been shown to have excellent abilities in optimizing multi-dimensional and multi-objective problems. The basic pseudo code for the PSO algorithm, given by [13].

In order to solve any problem with PSO, we need to define a fitness function which will be used to measure the quality of possible solutions for that problem. In antenna array problems, there are many parameters that can be used to evaluate function such as gain, side lobe level, and radiation pattern. Here, we are interested in designing a linear antenna array with minimum side lobes levels. Thus, the following fitness function is applied to the evaluation, defined as:

$$\text{fitness} = \min\left(\sum_{\varphi_i=\varphi_0}^{\varphi_i=\varphi_R}(\max \text{SLL}(\theta,\varphi_i))/R\right) \quad (35)$$

Where

max SLL : is the maximum sidelobe level of *linear antenna* array of 2N isotropic elements obtained by using PSO.
R: is the total sample point.
ϕ_i : are points where we have maximum sidelobe level
ϕ_0 : is initial value of azimuthal angle
ϕ_R : is maximal value of azimuthal angle

III. Numerical Results And Discussion

In order to investigate the accuracy of the theoretical formulation in previous section, we compared our results concerning superconducting rectangular microstrip antenna. Table 1 demonstrated relation between the real part of frequency resonance, bandwidth, and the thickness of superconducting film t of the antenna, is considered for four different relative permittivity of substrate. The superconducting material (YBCO) characteristics are: σn=210s/mm, l0=1500Å and T/Tc=0.5, a=1630μm, b=935μm, d=254μm. In table 1, it is observed that as the thickness of superconductor patch grows, the resonant frequency increases. These behaviors agree with those reported by Richard and all [4]. Also the numerical results show that, the antenna parameters (resonant frequency and bandwidth) do not vary significantly with the permittivity variation perpendicular to the optical axis (ex). Moreover, these are found to be strongly dependent with the permittivity (ez) is changed and (e1x) remains constant.

TABLE I: FREQUENCY RESONANT AND BANDWIDTH OF VARIOUS SUPERCONDUCTING RECTANGULAR MICROSTRIP

ε_x	ε_z	t(μm)	Resonant Frequency (GHz)	Bandwidth (%)
9,4	11.6	0.02	41.28	5.42
		0.08	41.36	5.37
		0.1	41.37	5.35
11.6	11.6	0.02	40.54	7.87
		0.08	40.61	7.76
		0.1	40.62	7.74
13	10.3	0.02	42.75	12.33
		0.08	42.81	12.21
		0.1	42.81	12.20
10.3	10.3	0.02	42.22	10.41
		0.08	42.91	09.12
		0.1	42.942	09.04

Table 2 summarizes the computed resonant frequencies for various perfectly rectangular microstrip. We have a perfectly conducting rectangular antenna, is printed on a substrate of permittivity e1x=e1z=2.33, with a thickness d=0.3175cm. The air gap has the effect of reducing the effective permittivity of the cavity beneath the patch, resulting rising shift in the resonant frequency. We compare our theoretical values for three different values of a and b, by using the full-wave moment method (MoM), with experimental data, which have been suggested in [14], note that the agreement is very good.

TABLE II: FREQUENCY RESONANT OF VARIOUS PERFECTLY RECTANGULAR MICROSTRIP ANTENNAS

a(cm)	b(cm)	h(mm)	Resonant frequencies (GHz)	
			Computed [11]	Our results
5.70	3.8	0.5	2.51	2.426
4.55	3.05	0. 5	3.05	2.976
2.95	1.95	0. 5	4.42	4.49

We consider reducing the sidelobe level in a linear array of the 8, 10 and 16 isotropic elements, which are non-uniform spacing and excitations of elements. In order to illustrate the capabilities of the particle swarm optimization (PSO) to find acceptable side lobe level (SLL), equal or less than the desired radiation pattern

The PSO program has been written in Matlab language, using 300 iterations. The number of particles taken is 200, the values of C1 and C2 are 2 respectively, and we have set (W1 = 0.9, W2 = 0.4). The minimum of fitness function values against number of generation is demonstrated in figure 3, for even number of elements positioned symmetrically along the x-axis. From this figure, it is clear that fitness function converges to optimal solution.

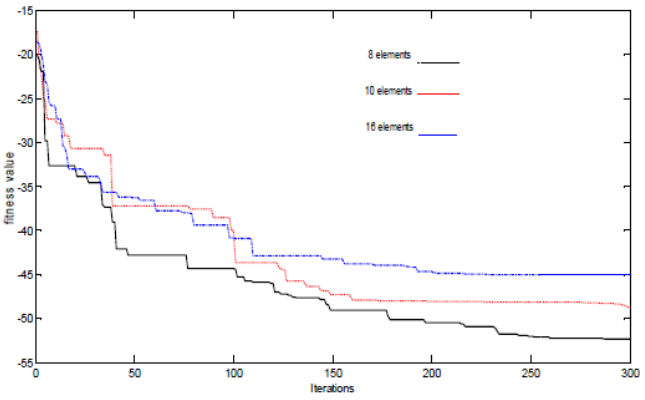

Fig. 3. Convergence curve of the fitness value of the 8, 10 and 16 elements linear array versus the number of iterations

The optimum parameters of amplitudes of excitation and positions obtained by our formulation using PSO can be utilizing to plot the variation of radiation patterns of linear array of (1, 8, 10 and 16) elements, which shown in Figures 5-8. Clearly, our results are generally better in terms of the sidelobe level and directivity of radiation pattern than those suggested by using Dolph-chebyshev distribution. This last distribution is considered as the optimal array for the uniform array, but the Dolph-Chebychev distribution also has uniform sidelobes. However, for some applications, a non-uniforme array is desirable. For the case of array of rectangular superconducting microstrips with multilayer dielectrics, the radiation patterns is calculated by using the product of the element factor Eq ,F. and the array factor AF(q ,f) .

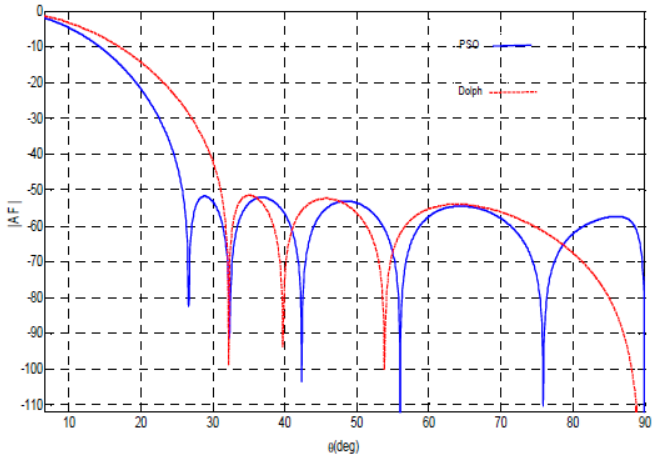

Fig. 4. Radiation pattern of linear array of 8 rectangular superconducting microstrip antenna versus angle θ

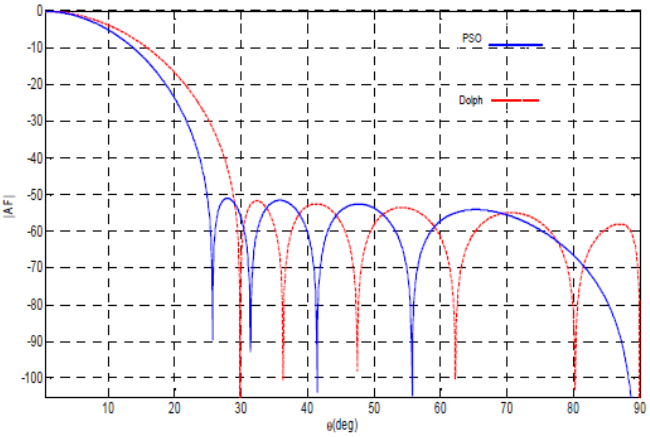

Fig. 5. Radiation pattern of linear array of 10 rectangular superconducting microstrip antenna versus angle θ

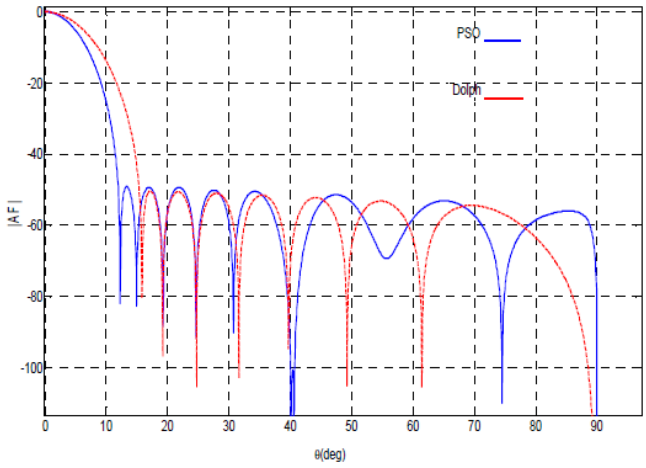

Fig. 6. Radiation pattern of linear array of 16 rectangular superconducting microstrip antenna versus angle θ

IV. Conclusion

The spectral domain and the stationary phase formulations have been used for the numerical calculation of the resonant frequency and radiated field of a of single rectangular microstrip antenna. The resolution of the integral equations of the electric field by the procedure of Galerkin makes it possible to lead to a system of equations homogenous. Variation of the resonant frequency versus the thickness of High superconducting rectangular microstrip on uniaxial substrate has been presented. In addition, we have presented an optimization technique based on particles swarm optimization algorithm, which is successfully used to determine the element excitations and positions of non-uniform linear antenna arrays, for simultaneous reduction of the side lobe level. The far field radiation patterns obtained by PSO algorithm are compared with the far field radiation patterns by Dolph-chebyshev distribution. A comparative study shows that PSO is capable of synthesising the unequally spaced linear antenna arrays to produce radiation patterns with a good performance in the sidelobe region.

References

[1] C. A. Balanis, Antenna theory: analysis and design. John Wiley and Sons, Hoboken, NJ, USA, 2005.

[2] J. R. James, P. S. Hall and C. Wood, Microstrip antenna theory and design,1981. https://doi.org/10.1049/PBEW012E

[3] L. H. Randy Antenna arrays: a computational approach. John Wiley & Sons, Inc, Hoboken, New Jersey, 2010.

[4] M. A. Richard, K. B. Bhasin, P. C. Claspy, “Superconducting microstrip antennasd: An experimental comparison of two feeding methods. IEEE Trans. Antennas Propagat;1993. Vol 41. N°7. p. 967-974. https://doi.org/10.1109/8.237630

[5] R. C. Hansen Electrically Small, Superdirective, and Superconducting Antennas, John Wiley& Sons, Inc, Hoboken, New Jersey; 2006. https://doi.org/10.1002/0470041048

[6] O. Barkat, A. Benghalia , “Radiation and resonant frequency of superconducting annular ring microstrip antenna on uniaxial anisotropic media,” Springer, Journal of Infrared, Millimeter, and Terahertz Waves, vol 30, N° 10, pp. 1053-1066, 2009. https://doi.org/10.1007/s10762-009-9526-2

[7] Z. Cai, J. Bornemann, “Generalized Spectral Domain Analysis for Multilayered Complex Media and High Tc Superconductor application,” IEEE Transactions on microwave Theory and Techniques, vol 40, N°12, pp. 2251- 2257, 1992. https://doi.org/10.1109/22.179887

[8] O. Barkat, “Modeling and optimization of radiation characteristics of triangular superconducting microstrip antenna array,” Journal of Computational Electronics, Springer, vol 13. N° 3. pp. 657–665, 2014. https://doi.org/10.1007/s10825-014-0584-x

[9] SO. Park, CA. Balanis, CR. Birtcher, “Analytical evaluation of the asymptotic impedance matrix of a grounded dielectric slab with roof top functions,” IEEE Trans Antennas Propagat, vol 46. N° 2. pp.251–259, 1998. https://doi.org/10.1109/8.660970

[10] J. R. Mohammed, “Phased Array Antenna with Ultra-Low Sidelobes,” Electronics Letters, vol 49, issue 17, pp. 1055-1056, August 2013. https://doi.org/10.1049/el.2013.1642

[11] J. R. Mohammed, “ Optimal Null Steering Method in Uniformly Excited Equally Spaced Linear Array by Optimizing Two Edge Elements,” Electronics Letters, vol 53, issue 11, 2017. https://doi.org/10.1049/el.2017.1405

[12] J. R. Mohammed, and K. H. Sayidmarie, “A Null Steering Method by Controlling Two Elements,” IET Microwaves, Antennas & Propagation, vol 8, issue 15, pp.1348-1355, 2014. https://doi.org/10.1049/iet-map.2014.0213

[13] O. Barkat, “Theoretical study of superconducting annular ring microstrip antenna with several dielectric layers,” Progress in electromagnetics research, vol 127, pp. 31-48. 2012. https://doi.org/10.2528/PIER12020105

[14] F. Abboud, J. P. Damiano, A. Papiernik, “Accurate model for the input impedance of coax-fed rectangular microstrip antenna with and without air gaps,” Proceedings of Sixth International Conference on Antennas and Propagation, vol 1, pp. 102-106, April 1989.